Accurate Measurement of Powder Diffraction Intensities Using Synchrotron Radiation*

W. Parrish[A] *and M. Hart*[B]

[A] Department K31/802, IBM Almaden Research Center,
650 Harry Road, San Jose, CA 95120–6099, U.S.A.
[B] Department of Physics, The University,
Manchester, M13 9PL, U.K.

Abstract

This paper reviews the advantages of synchrotron radiation for obtaining accurate values of the integrated intensities of powder samples for crystal structure refinement. The higher accuracy than conventional X-ray tube focusing methods results from the parallel beam geometry which has a symmetrical constant instrument function, higher intensity and resolution and easy wavelength selectivity. The importance of specimen preparation and the profile fitting function are discussed.

1. Introduction

Recent developments of synchrotron radiation powder diffraction methods have renewed interest in X-ray crystal structure refinement and determination using powder samples. Analyses using conventional X-ray tube focusing methods have had limited use and rather low precision mainly because of problems arising from the varying asymmetric profile shapes and the complex instrument function. In contrast, neutron diffraction powder data have simple Gaussian profile shapes and have been successfully used to determine hundreds of crystal structures by the Rietveld method.

The synchrotron radiation parallel beam powder method has a simple constant instrument function and the patterns have high peak-to-background. It has important advantages over neutrons in the much higher intensity which allows recording a high quality pattern for structure analysis in a few hours, and in the easy wavelength selectivity to optimise the experiment.

For a given $\sin\theta/\lambda$ range, single crystal diffraction patterns have many more reflections than powder patterns. A number of reflections are intrinsically superimposed in powder patterns (e.g. 333/511), and there are usually many overlaps forming clusters of reflections. The experimental data must, therefore, be of the highest quality to approach single crystal analysis. Two related factors are also of the highest importance, the specimen preparation and the profile fitting procedure. These topics form the subject of this paper.

A number of structures have been solved recently using different synchrotron radiation powder methods. Attfield *et al.* (1986) used a fibre specimen and crystal analyser, Lehmann *et al.* (1987) used a fibre specimen with linear position sensitive proportional counter and Will *et al.* (1988) used a flat specimen with long parallel slits,

---

* Paper presented at the International Symposium on Accuracy in Structure Factor Measurement, held at Warburton, Australia, 23–26 August 1987.

as described in Section 2. Although the methods are relatively new the patterns are far superior to those obtained with conventional X-ray tube methods. The experimental methods and profile fitting procedures will likely be further improved and with better specimen preparation we can expect a large increase in powder structure analysis using synchrotron radiation.

2. Experimental Methods

The experimental methods used in this paper have been described elsewhere (Parrish and Hart 1985; Parrish 1988). The silicon (111) channel monochromator used allows wavelength selection from the continuous storage ring radiation without changing the alignment or calibration of the powder diffractometer. The useful range is about $0 \cdot 5$ to 2 Å. Wavelengths can be chosen to obtain the highest peak-to-background and to avoid or minimise fluorescence background. The long distance between specimen and detector also suppresses the recorded fluorescence without the intensity loss caused by a diffracted beam monochromator. Because of the high resolution and symmetrical
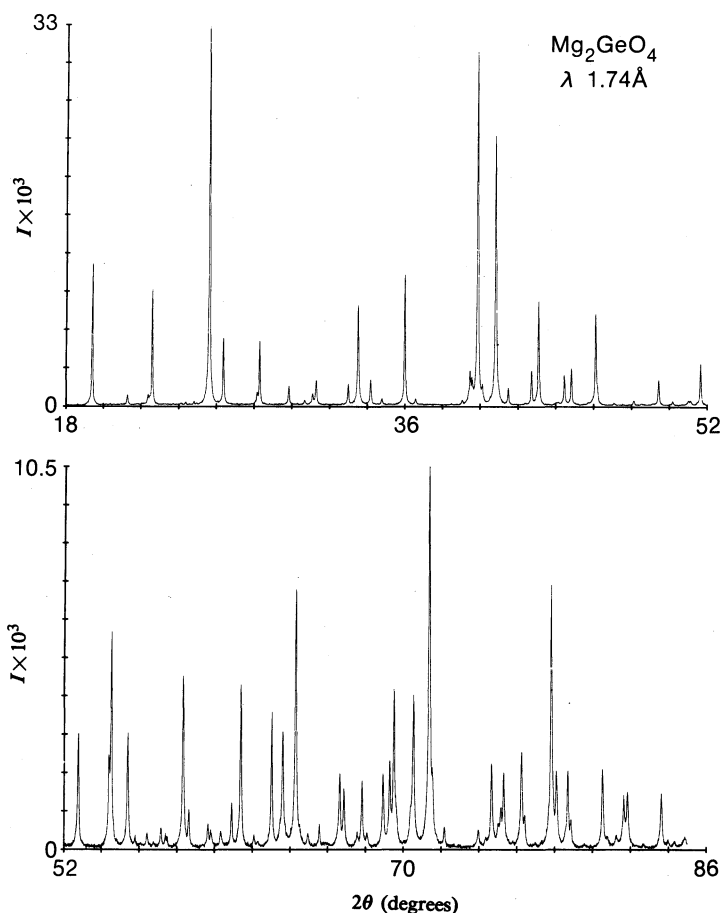

Fig. 1. Synchrotron radiation high resolution powder pattern of Mg_2GeO_4, with $\lambda = 1 \cdot 74$ Å, a d range of $5 \cdot 56$–$1 \cdot 27$ Å, $\Delta 2\theta = 0 \cdot 01°$, $t = 2$ s, and a resolution of $0 \cdot 05°$.

profile shapes, short wavelengths can be used to condense the pattern and reduce the recording time without loss of quality; very small *d* values can be reached if desired. Long wavelengths are used to increase the peak separations and aid in the profile fitting of complicated overlapping patterns. Wavelengths close to an absorption edge are available for anomalous scattering investigations. The crucial point is the easy selectivity to optimise the experimental data for all types of studies.

The resolution is determined by a set of 35·6 cm long Soller slits with 0·064° full aperture. The full width at half maximum (FWHM) of the profiles is 0·05° and increases with tanθ due to wavelength dispersion. The diffractometer gears must have high precision and reproducibility to avoid intensity errors in the very narrow peaks. An example of the high quality diffraction patterns that can be obtained with the method is that of orthorhombic Mg_2GeO_4 shown in Fig. 1. The high resolution combined with the 1·74 Å radiation and low uniform background resolved most of the 81 peaks and the remaining peaks could be easily separated by profile fitting. It was also easy to identify the minor second phase produced during the synthesis of the material.

Computer control of the step scanning permits selection of step increments $\Delta 2\theta$ and counting time *t*. There is no difference in the counting statistical accuracy as to how $\Delta 2\theta$ and *t* are proportioned, providing they are reasonable and fit the total available time. For patterns with no or little overlapping, $\Delta 2\theta$ can be 0·02° to 0·03° with no loss of precision if there are a sufficient number of points per peak for profile fitting. Regions of severely overlapped reflections require 0·01° or smaller steps for maximum recording resolution. The count time is decided by the time available for the experiment.

There is always the possibility of a beam loss which would interrupt the recording and require scaling with the section run after the beam was restored. It is generally
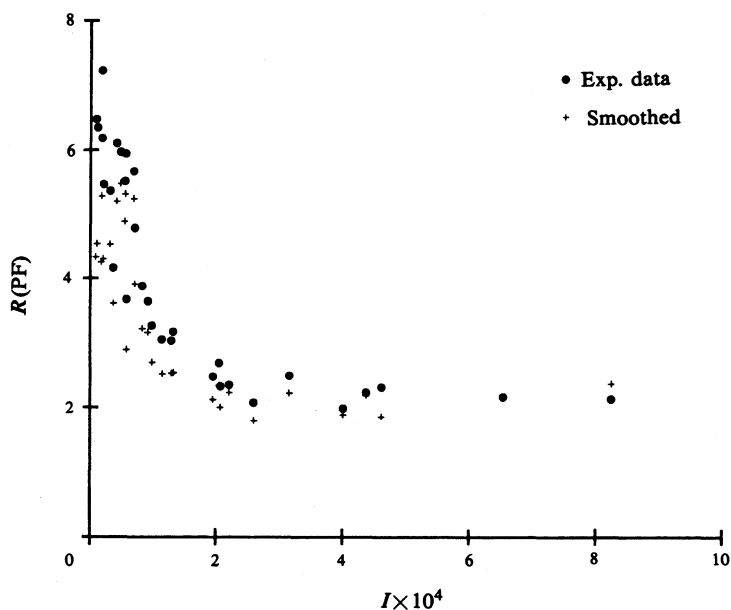

Fig. 2.   Variation of *R*(PF) with intensity, for quartz powder data.

better to make a number of recordings with short t values and to add them for data analysis. At least some of the runs are then likely to be usable.

The usual counting statistical rules apply. Although the intensities are higher than those from X-ray tubes there are often weak peaks and overlapped sections which require better data to improve the analysis, and may require reruns with increased counting time. The goodness-of-fit R(PF) (described in Section 4) is dependent on the intensity, as shown in Fig. 2. As the number of counts in a peak increases R(PF) decreases. There is no further improvement beyond a certain intensity and the limiting value appears to be the profile fitting function used. It makes no difference if raw or smoothed data are used because the profile procedure is automatically a smoothing process.

3. Specimen Quality

The theory of powder diffraction assumes that the specimen is made of a large number of small equal size particles in completely random orientation. In practice this is difficult to achieve and the quality of the specimen is often the most important
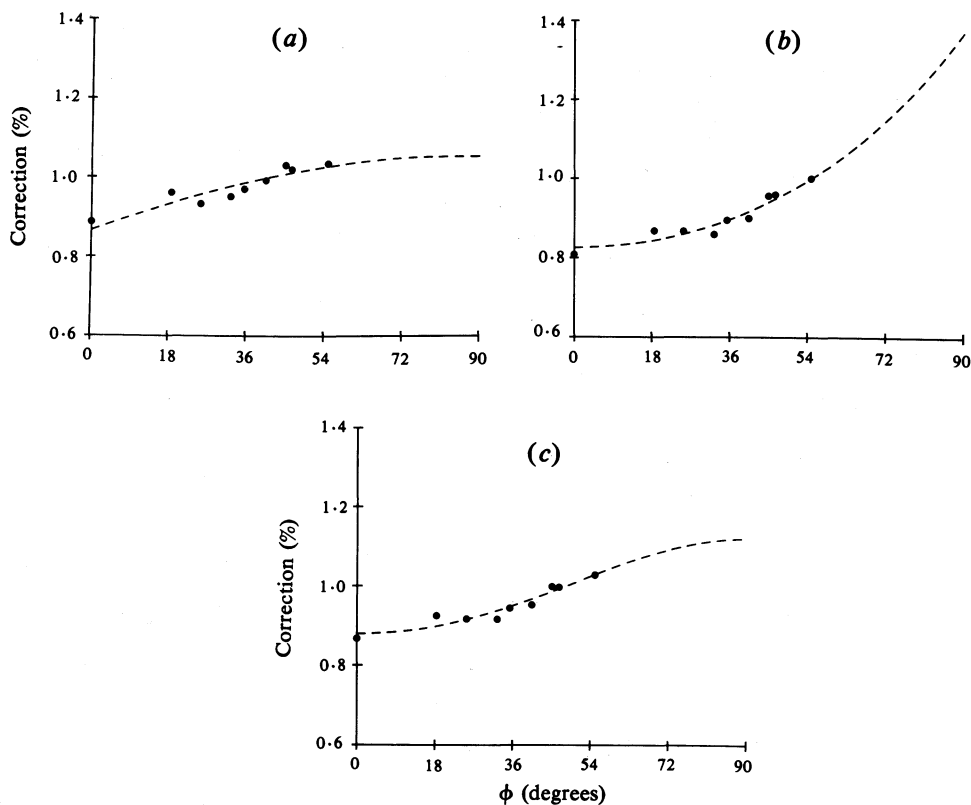
Fig. 3. Functions (dashed curves) used to correct the data for non-random orientation: (a) $P(hkl;\phi) = \exp(- GP\phi^2)$; (b) $P(hkl;\phi) = \exp\{ GP(\frac{1}{2}\pi - \phi^2)\}$; and (c) $P(hkl;\phi) = (GP^2\cos^2\phi + \sin^2\phi/ GP)^{-3/2}$. Experimental points are for silicon powder, with preferred orientation plane of (100).

factor limiting the precision of the intensity data. Although it is still more an art than a science, high quality specimens can be prepared with reasonable care.

The parallel beam geometry requires the particles to be in the exact orientation to reflect. The number of correctly oriented particles is much smaller than in conventional focusing geometry where particles oriented within the range of the angular apertures can reflect. Our experience shows that it is necessary to use <10 μm powder to achieve good particle statistics (Parrish *et al.* 1986). Very small particles <1 μm cause profile broadening which may be a problem in resolving closely spaced overlaps. We have used a motor-driven oscillating vial containing the powder and a hard sphere for grinding, and an acoustically-driven Lektromesh screen for sifting. It is a long and tedious process and when possible it is better to obtain small particles in the chemical preparation.

The specimens are prepared as flat circular surfaces of 22 mm diameter, using amyl acetate-collodion as a binder. Others (Cox 1987) have used a fibre or capillary specimen mount which is stated to have less preferred orientation and seals it from the environment. However, the intensity is reduced by the smaller powder volume and absorption corrections are necessary.

Rotating the specimen about 70 r.p.m. around the axis normal to the surface greatly improves the particle size statistics by bringing many more particles into reflecting positions (Parrish and Huang 1983). Oscillating the specimen over a small angular range has been used (Yukino and Uno 1986). We have found little difference between rotation and rotation combined with oscillation.

Even with careful specimen preparation it is still difficult to achieve completely random orientation. This leads to errors in the relative intensities which appear as errors in the structure refinement. It is, therefore, necessary to use an empirical correction factor determined by ϕ, the acute angle between the plane of 'preferred orientation' and the diffracting plane *hkl*:

$$I(\text{corr}) = I(hkl)\,P(hkl)(\phi). \tag{1}$$

Three functions have been used and are shown in Fig. 3. The preferred orientation plane was selected by trial and error using a fast routine with only seven cycles in the powder least squares structure refinement. The first dozen reflections were used and the plane which gave the lowest R(Bragg) value was selected as the plane of preferred orientation. By including the correction in the structure refinement the R(Bragg) value for silicon decreased to 0·75% from 3·5% and for Mg_2GeO_4 to 4·9% from 12·5%.

4. Profile Fitting

In crystal structure determination the integrated intensities are required rather than the peak values. They are obtained from a profile fitting procedure in which a predetermined function is fitted to the experimental data points. The differences of intensities between points on the fitted curve at the same angular positions as the points on the experimental curves determine the goodness of fit

$$R(\text{PF}) = \left\{ \left(\sum_{i=1}^{n} \{ Y_i(\text{obs}) - Y_i(\text{calc}) \}^2 \right) \bigg/ \sum_{i=1}^{n} Y_i(\text{obs})^2 \right\}^{\frac{1}{2}} \times 100\% . \tag{2}$$

Isolated high intensity peaks usually have $R(PF) = 1–2\%$ which may increase to 2–8% in low intensity overlapping peaks.

The observed profile is a convolution of three terms: the incident spectral distribution, the shape and aberrations produced by the instrument geometry, and the broadening caused by the specimen. The first two define the instrument function and are the same in all patterns recorded with the same X-ray optics. The instrument function can be measured using a specimen free of profile broadening and having well separated high intensity reflections. We used a silicon powder standard (National Bureau of Standards 640a; Hubbard 1983) or a mixture of silicon and tungsten. These standards have additional advantages: the data can be used to determine the lattice parameter by least squares refinement and simultaneously the correction of the diffractometer zero-angle position. They also provide a check on the instrumentation and wavelength setting of the monochromator. If a sample with broadened peaks is to be analysed, isolated reflections of the actual specimen must be used to determine the best fitting function.
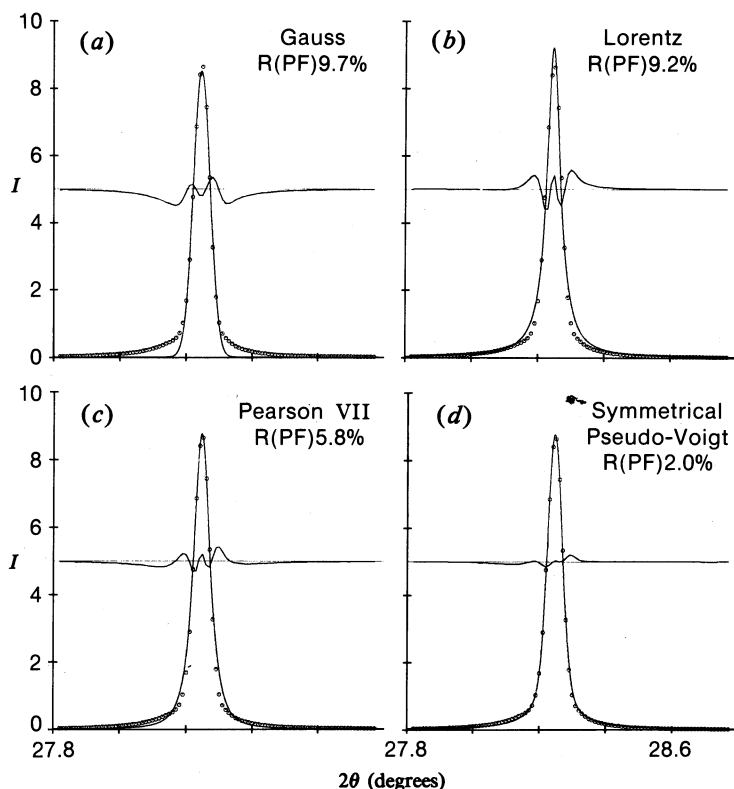

Fig. 4. Profile fitting functions. Experimental data points are for Si(111), $\Delta 2\theta = 0\cdot01°$, 38 K counts at peak and $\lambda = 1.54$ Å. The observed–calculated differences are also shown at half height.

There is no universal profile shape function and it must be carefully determined for each instrument arrangement. Four commonly used functions are shown by the curves in Fig. 4. The experimental points are from the silicon (111) peak. The

differences between experimental and profile fitted data points are also shown at half
height. Poor fitting of the peak and tails of the pure Gauss, Lorentz and the Pearson
VII caused the large $R(PF)$ values indicated.

The smallest residual was obtained with the pseudo-Voigt function defined as

$$pV = \eta L + (1-\eta) G, \tag{3}$$

where L and G are the Lorentz and Gaussian components and η is the ratio L/G.
The variables to be refined are the position $2\theta_{peak}$, intensity I_{peak} and the FWHM
of the L and G components. The widths can be independently refined holding η
constant, or vice versa; we obtained better results with the former. A silicon dataset
was refined by systematically varying η. For the instrument geometry used $\eta = 0.25$
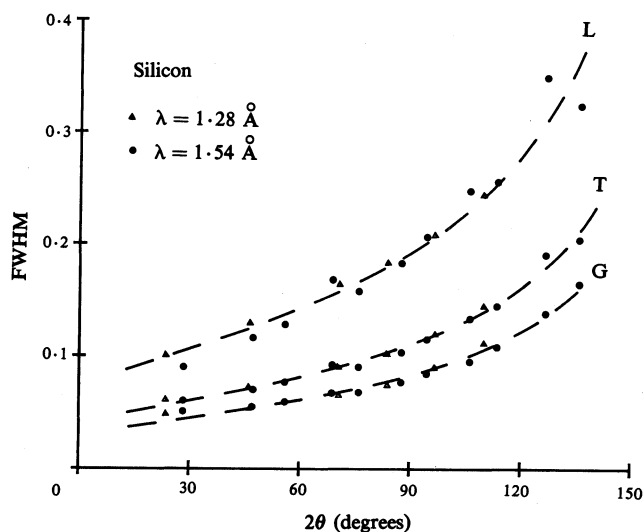gave the lowest $R(PF)$ value, i.e. the sum of $25\% L + 75\% G$.

Fig. 5. Profile width increase with $\tan\theta$, where L is the Lorentzian component,
G the Gaussian and T the total profile, for silicon powder data with two
wavelengths.

The FWHM of a pseudo-Voigt function increases with increasing scattering angle.
The Gaussian component width is given by (Attfield *et al.* 1986)

$$(\text{FWHM})_G = (U \tan^2\theta + V \tan\theta + W)^{\frac{1}{2}}, \tag{4}$$

and the Lorentzian component by

$$(\text{FWHM})_L = X \tan\theta = Y/\cos\theta. \tag{5}$$

The total width is the sum of the G and L widths which were separately determined.
The angular dependence is shown in Fig. 5 for a silicon powder dataset. The dashed
$\tan\theta$ curves show the effect of wavelength dispersion. The coefficients may vary with
the specimen characteristics. It is generally assumed that small crystallite sizes add to
the Lorentzian component and microstrains to the Gaussian (de Keijser *et al.* 1982).

   If the peaks are asymmetric different half-widths can be used for the right and left sides of each component, thus adding two variables to the refinement. The $R(PF)$ values shown no dependency on scattering angle but there was a large dependence on intensity as would be expected. The $R(PF)$ value decreased from 7% to 2·5% when the intensity increased from 10^2 to 10^4 counts, and remained constant at 2% for the higher intensities. Nevertheless, useful data can be obtained from even very weak peaks.

   The integrated intensities were calculated from the following expressions:

$$I(G)_{\text{integ}} = (1-\eta)_{\text{peak}}(\text{FWHM})_G\,(\pi/4\ln2)^{\frac{1}{2}} \qquad (6)$$

for the Gaussian component, and

$$I(L)_{\text{integ}} = \eta\,I_{\text{peak}}(\text{FWHM})_L\,(\pi/2)^{\frac{1}{2}} \qquad (7)$$

for the Lorentzian. The integrated intensity of the total curve is the sum of both. The intensity values can be checked by adding the counts of the individual points. The numerical integration value is slightly higher than the profile fitted value because of the long tails of the Lorentzian component.

   The determination of the individual intensities of overlapping reflections is easy to do if the angular separation of the peaks exceeds the individual FWHM values. If the separations are smaller, least-squares ill-conditioning may be caused by the correlation between position and intensity of adjacent peaks and may lead to relatively large errors. Several methods have been used to circumvent this problem. The scattering angles calculated from the lattice parameter may be entered in the program to specify the peak positions in the cluster. The Pawley (1981) method may be tried in which slack constraints are used to determine the intensity differences. We have also successfully used the total intensity of the cluster of very closely overlapped peaks in the powder least-squares refinement program (Will *et al.* 1987). Although the individual $R(PF)$ values may be large, the overall fitting of the cluster can be good as shown by the difference curve.

5. Conclusions

   High quality powder diffraction patterns with sufficient precision for crystal structure determination can be obtained with the new synchrotron radiation parallel beam method. The method has many advantages over X-ray tube focusing methods: higher intensity and resolution, symmetrical profiles, simple constant instrument function and easy wavelength selectivity. Careful specimen preparation using <10 μm powder and corrections for non-random orientation are essential. There is no universal profile fitting function and it must be carefully determined for each instrument geometry.

   An example of the precision achieved in crystal structure refinement is the result for quartz, a simple structure with few positional parameters. The highest/lowest intensities had a range of 4600:1. The $R(\text{Bragg})$ value was 1·60, the same as obtained in single crystal refinement. The estimated standard deviations of the positional parameters were 2·5 times larger than the single crystal results which had a 9 times larger dataset.

References

Attfield, J. P., Sleight, A. W., and Cheetham, A. K. (1986). *Nature* 322, 620–2.

Cox, D. E. (1987). *Mater. Res. Bull.* 12, 16–20.

de Keijser, T. H., Langford, J. I., Mittemeijer, E. J., and Vogels, A. B. P. (1982). *J. Appl. Crystallogr.* 15, 308–14.

Hubbard, C. R. (1983). *Adv. X-ray Anal.* 26, 45–51.

Lehmann, M. S., Christensen, A. N., Fjellvag, H., Fiedenhans'l, R., and Nielsen, M. (1987). *J. Appl. Crystallogr.* 20, 123–9.

Parrish, W. (1988). *Aust. J. Phys.* 41, 101.

Parrish, W., and Hart, M. (1985). *Trans. Am. Crystallogr. Assoc.* 21, 51–5.

Parrish, W., Hart, M., and Huang, T. C. (1986). *J. Appl. Crystallogr.* 19, 92–100.

Parrish, W., and Huang, T. C. (1983). *Adv. X-ray Anal.* 26, 36–44.

Pawley, G. S. (1981). *J. Appl. Crystallogr.* 14, 357–61.

Will, G., Bellotto, M., Parrish, W., and Hart, M. (1988). *J. Appl. Crystallogr.* 21 (in press).

Will, G., Masciocchi, N., Parrish, W., and Hart, M. (1987). *J. Appl. Crystallogr.* 20, 394–401.

Yukino, K., and Uno, R. (1986). *J. Appl. Phys. Jpn* 25, 661–6.